JOC The Journal of Organic Chemistry

Article

pubs.acs.org/joc

α-Phenyl-*N*-cyclohexyl Nitrones: Preparation and Use as Spin-Traps

Grégory Durand,*[,†] Marie Rosselin,[†] Pierre-André Klein,[‡] Kamal Zéamari,[†] Fanny Choteau,[†] and Béatrice Tuccio[‡]

[†]Institut des Biomolécules Max Mousseron UMR 5247 CNRS-Université Montpellier-ENSCM & Avignon Université, Equipe Chimie Bioorganique et Systèmes Amphiphiles, 301 rue Baruch de Spinoza BP 21239, Avignon 84916 Cedex 9, France

[‡]Aix-Marseille Université, CNRS, ICR (UMR 7273), Marseille 13397, France

Supporting Information

ABSTRACT: Two bifunctional α-phenyl-*N*-cyclohexyl nitrones were synthesized with the expectation that the cyclohexyl ring will impart lipophilicity to the molecule, high reactivity to the nitronyl group, and stability to the spin adducts formed. The synthesis of the acid nitrone **4** and its corresponding *tert*-butyl ester **3** was initiated by a Michael reaction to introduce the cyclohexyl ring. A Zn/AcOH-mediated reduction of the nitro functionality followed by condensation onto benzaldehyde generated the nitronyl function. In agreement with their high lipophilicity values, nitrone **3** was insoluble in water, while nitrone **4** exhibited a poor water solubility. It was determined that the presence of the cyclohexyl ring did not affect either the reduction or oxidation potentials of the nitronyl group in comparison to the classical α-phenyl-*N*-*tert*-butylnitrone (PBN). The spin trapping ability of **3** and **4** was investigated by EPR for oxygen- and carbon-centered radicals. In most cases, the nitrones gave rise to a standard six-line EPR spectrum whose values were in agreement with the literature, accompanied by a minor second species. In DMSO, the half-lives of nitrone **3** and **4**–OOH adducts were double that of PBN, suggesting that the stabilization comes from the cyclohexyl ring and/or the electronic effect of the carboxylic acid.

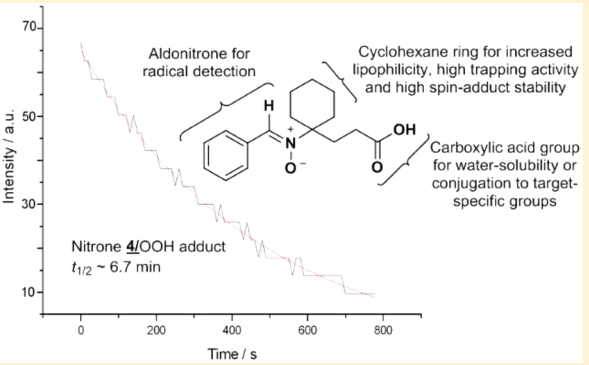

INTRODUCTION

Nitrone-based compounds have been widely used as spin-traps for detecting transient free radicals. The nitronyl group reacts with a free radical to form a stable and identifiable aminoxyl radical that can be detected by electron paramagnetic resonance (EPR) spectroscopy.[1,2] Two families of nitrones are commonly employed: the cyclic nitrones derived from the 5,5-dimethyl-1-pyrroline *N*-oxide (DMPO) and the linear variants derived from the α-phenyl-*N*-*tert*-butyl nitrone (PBN). Aside from their use as spin-traps, the ability of nitrones to prevent oxidative stress-mediated damage in in vitro, in vivo, and ex vivo models has made them promising synthetic antioxidants with considerable potential as therapeutics.[3−6]

When used as probes, it is of the utmost importance to design nitrone spin traps that have the highest rate constant of free-radical trapping to ensure efficient detection. The ease of free-radical detection is also determined by the stability of the corresponding aminoxyl spin adduct. In general, cyclic nitrones lead to longer lived adducts than linear ones, and therefore, several analogues of DMPO with improved persistence have been designed.[1] The phosphorylated analogue 5-(diethoxyphosphoryl)-5-methyl-1-pyrroline *N*-oxide (DEPMPO),[7] ester 5-(ethoxycarbonyl)-5-methyl-1-pyrroline *N*-oxide (EMPO),[8] 2-(*tert*-butoxycarbonyl)-5-methyl-1-pyrroline *N*-oxide (BocMPO),[9] amido derivative (AMPO),[10,11] and the trifluoromethyl analogue of DMPO (5-TFDMPO)[12] are illustrative examples. On the other hand, efforts to synthesize analogues of PBN with improved adduct stability have been met with limited success when compared to their cyclic counterparts.[13−15] In our group, a series of para- and *N*-*tert*-butyl-substituted PBN derivatives have been prepared. Although some of our derivatives proved more potent than PBN, their rate of trapping remained within the same order of magnitude.[16−18] In comparison to cyclic nitrones, linear nitrones are easier to synthesize and are often solid at room temperature, affording paramagnetic impurity free samples via recrystallization.

Several cyclic variants of PBN have been reported and examined as spin-traps and/or therapeutic agents. Thomas and colleagues reported the synthesis of 3,3-dimethyl-3,4-dihydroisoquinoline *N*-oxide (MDL 101,002, Figure 1) and several analogues where the presence of the ring system made the nitronyl group more reactive toward radicals due to restricted rotation and higher accessibility.[19,20] They also reported that, in comparison to PBN, their lead compound displayed high energy HOMO and lying energy LUMO orbitals, increasing its reactivity toward electrophilic and nucleophilic radicals.[19,20] Hideg and colleagues also reported a series of cyclic variants of

Received: September 14, 2016
Published: December 7, 2016

DOI: 10.1021/acs.joc.6b02262
J. Org. Chem. 2017, 82, 135−142

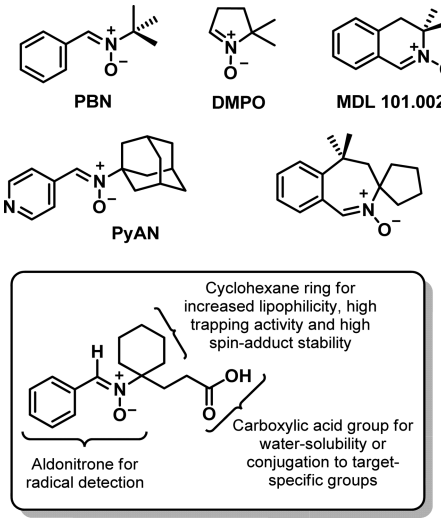

Figure 1. Structure of PBN and DMPO, representative cyclic variants of phenyl and aryl nitrones, and the general concept of α-phenyl-*N*-cyclohexyl nitrone.

PBN derived from adamantane (PyAN, Figure 1) whose hydroxyl adduct stability was increased for the most efficient derivative by ∼7 times when compared to that of PBN.[21,22] A heteroarylnitrone containing a *N*-cyclohexyl group showed interesting antioxidant properties, although surprisingly, it failed to show detectable HO• adduct signals while its *N*-*tert*-butyl analogue did.[23] A series of spirocycle-containing 2-benzazepine derivatives (Figure 1) were investigated for their ability to protect neuronal cells against oxidative stress. These compounds out performed PBN, presumably due to their increased lipophilicity.[24] A DMPO derivative with a rigid spirolactonyl moiety was also prepared and showed a higher rate constant of superoxide trapping compared to several DMPO analogues.[25]

In connection with our program devoted to the design of selectively targeted nitrone-based spin-traps with improved reactivity toward free radicals, we report herein the design of bifunctional α-phenyl-*N*-cyclohexyl nitrones (Figure 1). We anticipate that the cyclohexyl ring will increase lipophilicity and will increase the reactivity of the nitronyl group and stability of the resulting spin adducts. Further functionalization of the nitrone to accommodate target-specific groups may also impart high reactivity toward radicals, yield a longer adduct half-life, and afford enhanced and controlled bioavailability in a unified molecular design (Figure 1). The synthesis of the α-phenyl-*N*-cyclohexyl nitrone **4** and its corresponding *tert*-butyl ester **3** is described in this paper, and the water solubility, lipophilicity, and electrochemical properties of these two derivatives were determined. The spin-trapping ability of the two nitrones was next investigated by EPR, and the rate constants of superoxide radical anion and hydromethyl radical spin-adduct formation were experimentally determined.

RESULTS AND DISCUSSION

Synthesis. The synthesis of nitrone **4** began with a Michael reaction between nitrocyclohexane and *tert*-butyl acrylate (Scheme 1). After optimization (Table S1), it was found that a 1/35 mixture of KOH/MeOH in dry Et_2O as described by Kolter et al. was the most effective,[26] leading to compound **1** in 90% yield after flash chromatography purification. When *t*BuOK was used as a base, larger amounts of *tert*-butyl acrylate were needed to ensure a reasonable yield. Moreover, degradation of the reaction mixture was observed in some cases, with no compound **1** being formed. The next step required formation of the nitronyl group. We investigated two synthetic strategies. The first synthetic route relied on the reduction of the nitro group to its hydroxylamine form, which was further purified and isolated. Reduction was conducted in the presence of zinc dust and NH_4Cl in a 3:1 THF/H_2O mixture (v/v) under argon atmosphere following our previously reported procedure.[27] Hydroxylamine **2** was obtained in 80% yield and was then condensed with benzaldehyde under argon atmosphere in a dry 3:2 THF/AcOH mixture (v/v) in the presence of molecular sieves to give nitrone **3** in 92% yield. The second synthetic route consisted of a one-pot reduction–condensation of the nitro derivative **1** onto benzaldehyde in the presence of zinc dust and AcOH in EtOH.[28] Under these conditions, nitrone **3** was isolated after purification in 30% yield, and although this second strategy was one step shorter, it failed to bring any improvement in the overall yield. Finally, removal of the *tert*-butyl protecting group under acidic conditions led to nitrone **4** in 92% yield. It is worth noting that despite the use of TFA no degradation of the nitronyl group was observed. The synthesis of nitrone **4** was achieved in 61% overall yield in four steps, allowing gram-scale preparation.

Scheme 1. Synthesis of Nitrones 3 and 4

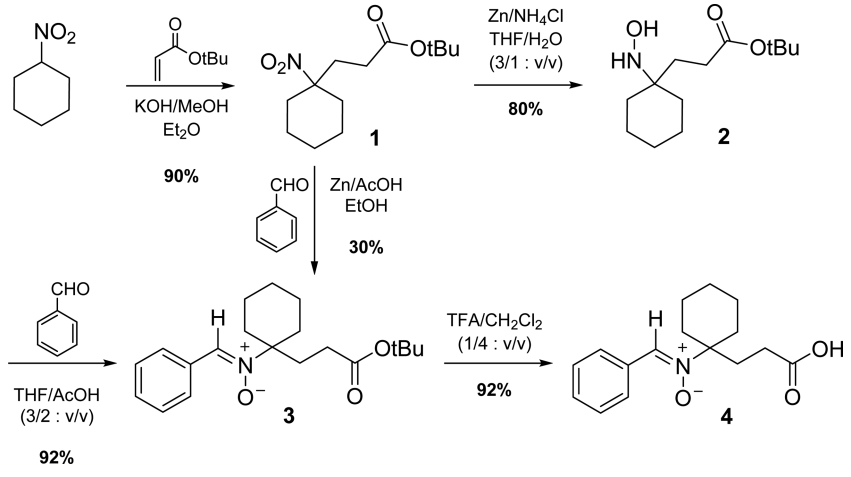

DOI: 10.1021/acs.joc.6b02262
J. Org. Chem. 2017, 82, 135−142

Table 1. Physical−chemical and Electrochemical Properties of Nitrones 3 and 4

		lipophilicity		E_p(c) (V)		E_p(a) (V)
nitrones	water solubility (g/L)	log $k'w$[c]	C log P[d]	in H_2O[e]	in CH_3CN[f]	in CH_3CN[f]
3	*a*	3.56	4.53	*a*	−2.19; −2.07	1.56
4	2.1 (17.1)[b]	2.32	3.33	−1.90	−2.28; −2.12	1.62
PBN	21.4	1.68	2.66	−1.74	−2.23; −2.04	1.61
				(−1.53; −1.94)	(−2.22; −2.12)	(1.53; 1.67)

[a]Not soluble. [b]Carboxylate form. [c]Partition coefficient values obtained by HPLC. [d]Calculated octanol/water partition coefficient values obtained using Marvin software (http://www.chemaxon.com/marvin/help/index.html). [e]Containing 50 mM of NaCl with reduction E_p(c) at Cv vitreous carbon electrode. [f]Containing 50 mM of TBAP with reduction E_p(c) and oxidation E_p(a) at Cv vitreous carbon electrode.

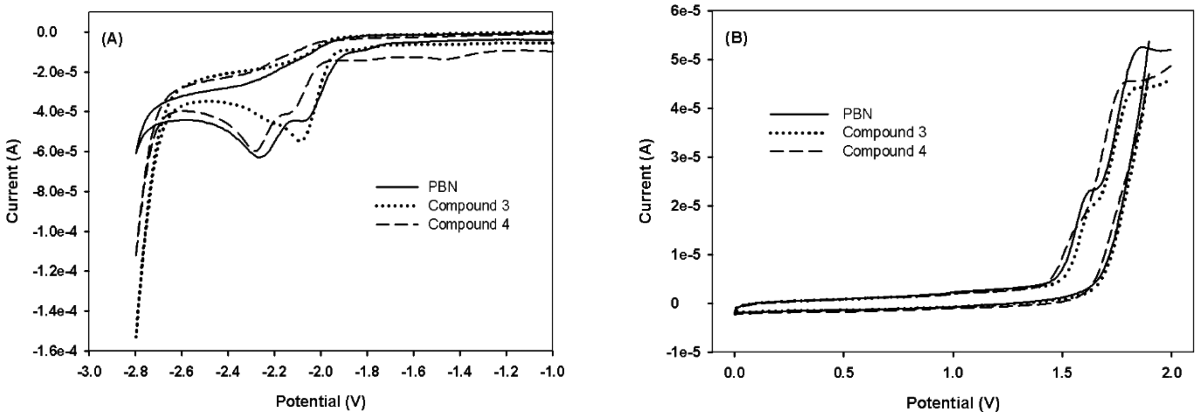

Figure 2. Cyclic voltammograms of PBN and nitrones **3** and **4** in acetonitrile containing 50 mM of TBAP with a sweep rate of 0.1 V·s^{-1}: (A) reduction and (B) oxidation.

Table 2. Hyperfine Coupling Constants Determined for a Series of Radical Adducts Obtained from the β-Substituted Nitrones 3 and 4

radical adducts			nitrone **3**			nitrone **4**			
radical	source	solvent	a_N	a_H	ratio (%)	a_N	a_H	ratio (%)	nitroxide detected
•OMe	$PbOAc_4$	MeOH	13.90	2.80		14.10	2.90	100	**3**-OMe or **4**-OMe
•$CH_2C(O)CH_3$	Fenton	acetone	13.97	3.72		14.18	3.57	64	**3**-$CH_2C(O)CH_3$ or **4**-$CH_2C(O)CH_3$
			13.97		32	14.23		36	unidentified nitroxide
•CH_2OH	Fenton	MeOH	15.15	4.16		15.26	4.41	63	**3**-CH_2OH or **4**-CH_2OH
			15.14		34	15.26		37	unidentified nitroxide
•$CH(CH_3)OH$	Fenton	EtOH	14.24	3.43		14.97	3.93	72	**3**-$CH(CH_3)OH$ or **4**-$CH(CH_3)OH$
			14.03		35	14.68		28	unidentified nitroxide
•CH_3	Fenton	DMSO	14.53	3.67		14.80	4.02	60	**3**-CH_3 or **4**-CH_3
			14.49		29	14.67		40	unidentified nitroxide
•O*t*Bu	(*t*BuO)$_2$, hν	CH_2Cl_2	13.80	2.14		13.73	2.10	67	**3**-OtBu or **4**-OtBu
			13.59	2.69	34	13.98	3.07	33	**3**-O_2Me or **4**-O_2Me
•O_2H	DTPA, riboflavin, blue light	DMSO	13.16	1.15		13.61	1.15	55	**3**-O_2H or **4**-O_2H
			13.62	3.88	39	14.39	3.05	45	C-centered radical adduct derived from **3** or **4**
H	$NaBH_4$, air	MeOH	15.30	9.72 (2H)		15.40	10.35 (2H)	80	**3**-H or **4**-H
			15.42	14.98	32	15.42	17.03	20	cyclic nitroxides

Before any physical−chemical investigation, both nitrones **3** and **4** were recrystallized twice in order to ensure high purity.

Water Solubility and Lipophilicity. The water solubility of nitrones **3** and **4** and their sodium salt was determined using the UV spectroscopy method[17] and was compared to that of PBN (Table 1). To prepare the salt, nitrone **4** was suspended in water and 1 N NaOH was added until pH ∼10, resulting in the complete dissolution of the nitrone. After filtration and lyophilization, the salt was obtained in quantitative yield. Nitrone **3** was insoluble in water while nitrone **4** exhibited a water solubility of 2.1 g/L, which is 10 times lower than that of PBN (21.4 g/L). Water solubility of nitrone **4** was significantly improved after conversion to its carboxylic salt form (17.1 g/L). The relative lipophilicity (log k'_w) of the nitrones was measured by HPLC, and the values are reported in Table 1. This confirmed the higher lipophilic character of the ester nitrone **3** compared to nitrone **4** with log k'_w values of 3.56 and 2.32, respectively, whereas the log k'_w found for PBN (1.68) was in agreement with previous reports.[27] Calculated partition coefficients (C log P) were also determined using Marvin software, and a good correlation was observed between the experimental and the calculated data (R^2 > 0.999, Figure S15).

DOI: 10.1021/acs.joc.6b02262
J. Org. Chem. 2017, 82, 135−142

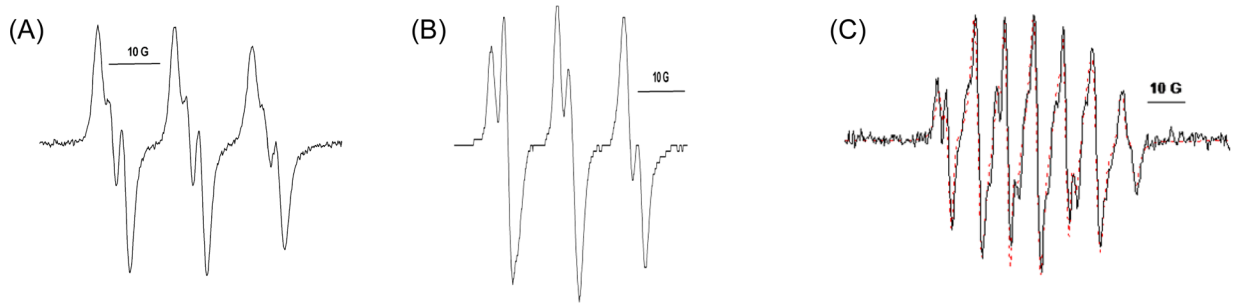

Figure 3. EPR spectra of (A) **3**−CH_2OH adduct obtained by using a Fenton system in water/methanol, (B) of **4**−O_2H adduct obtained by using a light/riboflavin/electron donor system in DMSO, and (C) **3**-H recorded after $NaBH_4$ reduction of **3** in methanol and the superimposed simulation (red dotted line). The various hfcc values obtained after simulation are given in Table 2.

Scheme 2. (A) Formation of Nitroxides 3-*3* and 4-*4* after Reaction of HO$^\bullet$ on Nitrones 3 and 4, Respectively; (B) Formation of Nitroxides 3-H and 4-H after a Forrester−Hepburn Mechanism and Proposed Mechanism for the Formation of Cyclic Nitroxides under the Basic Conditions of $NaBH_4$ Reduction

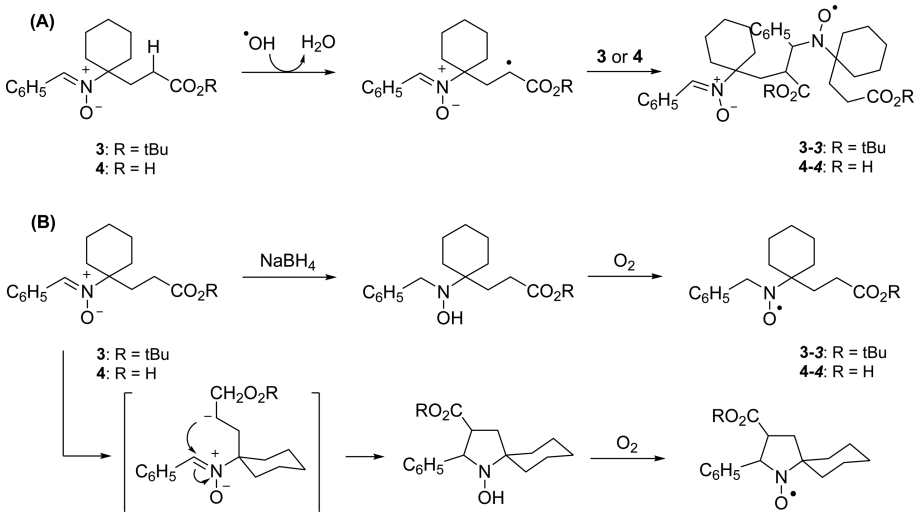

Cyclic Voltammetry. The electrochemical behavior of the two nitrones was investigated using cyclic voltammetry (Table 1). Initial cyclic voltammetry experiments were conducted in 50 mM NaCl aqueous solution. As previously observed for other nitrones, the oxidation of the nitronyl group was not measurable due to overlapping of the oxidation peak with the solvent discharge.[18,29,30] We have previously reported that para-substituted PBN derivatives possess two reduction peaks with the current of the first peak being much lower than the second one. In our hands, only one peak corresponding to reduction was observed, with a cathodic peak potential of −1.90 V vs Ag/AgCl for nitrone **4**, in comparison with PBN at −1.74 V. This shows that under aqueous conditions the reduction of nitrone **4** is less favored than that of PBN. It must also be noted that the reduction value observed for PBN correspond to the average of the two peaks observed in our previous work, i.e., −1.53 and −1.94 V. Due to its insolubility in water, nitrone **3** was not tested.

We next studied the electrochemical properties of the nitrones in acetonitrile containing tetrabutylammonium perchlorate (TBAP) as an electrolyte. PBN and nitrones **3** and **4** are reduced through two successive electron transfers in agreement with our previous observations (Figure 2A).[18] Only a modest ease of reduction was observed for nitrone **4** compared to nitrone **3** and PBN. Moreover, the two peaks are displaced toward negative potentials when the potential scan rate is increased (data not shown). Compared to the aqueous conditions, oxidation of nitrone **3** and **4** was clearly observed in acetonitrile (Figure 2B) with values of 1.56 and 1.62 V, respectively, compared with PBN at 1.61 V. This data shows that the presence of the cyclohexyl ring does not affect either the reduction or oxidation potentials of the nitronyl group, which is in agreement with findings by Zuman and Exner,[31] McIntire et al.,[29] and our group.[17] A thorough investigation of the redox properties of the two nitrones is beyond the scope of the current study.

Spin Trapping. To evaluate the spin-trapping ability of nitrones **3** and **4**, we investigated the formation of various carbon- and oxygen-centered radical spin adducts. The hyperfine coupling constants (hfcc's) are reported in Table 2, and examples of EPR spectra are presented in Figure 3. In most cases, the nitrones tested gave rise to a standard six-line EPR spectrum whose hfcc's are in agreement with the literature. Methoxy radical ($CH_3O^\bullet$) was generated in the presence of $PbOAc_4$ in methanol leading to a single species with hfcc values of a_N = 13.9 G and a_H = 2.8 G and a_N = 14.1 G and a_H = 2.9 G for nitrones **3** and **4**, respectively. Under the other conditions tested, two species were observed. The generation of the superoxide radical ($HO_2^\bullet/O_2^{\bullet-}$) was achieved by irradiation of a riboflavin solution in the presence of DTPA as a electron donor. For both nitrones, a major six-line species was observed and assigned to the nitrone−superoxide spin adduct. With this

DOI: 10.1021/acs.joc.6b02262
J. Org. Chem. 2017, 82, 135−142

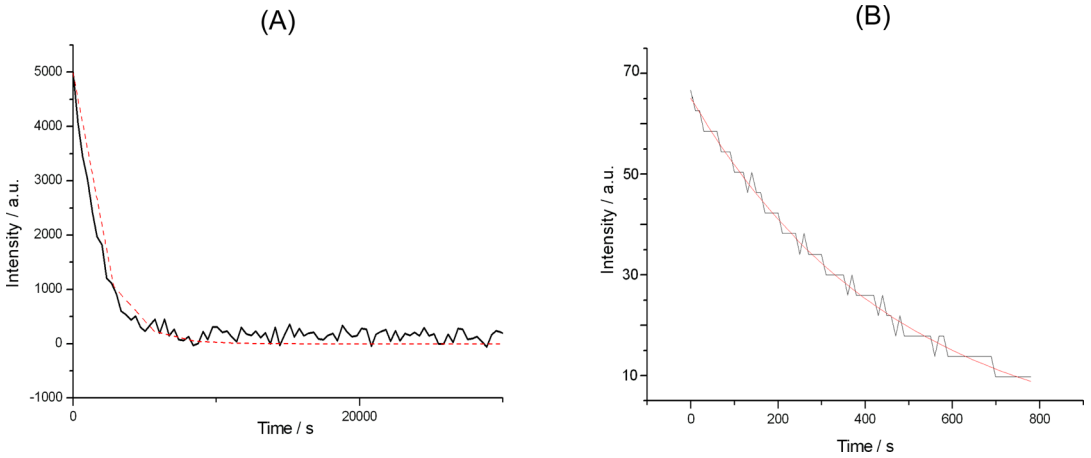

Figure 4. Experimental kinetic curve of decay of the adducts (black lines) and superimposed calculated curve (red dotted lines) obtained by considering a first-order decay: (A) **3**−CH_2OH adduct and (B) **4**−O_2H adduct. The kinetic parameters are given in Table 3.

Table 3. Half-life and Rate Constant of Decay for PBN, Nitrone 3, and Nitrone 4

	$^{\bullet}O_2H$		$^{\bullet}CH_2OH$	
	k_D (s^{-1})	$t_{1/2}$ (s)	k_D (s^{-1})	$t_{1/2}$ (s)
PBN	$(3.74 \pm 0.09) \times 10^{-3}$	185 ± 5	$(0.61 \pm 0.02) \times 10^{-3}$	1136 ± 38
nitrone **3**	$(2.12 \pm 0.14) \times 10^{-3}$	327 ± 24	$(0.54 \pm 0.02) \times 10^{-3}$	1284 ± 47
nitrone **4**	$(1.72 \pm 0.15) \times 10^{-3}$	403 ± 32	$(0.55 \pm 0.03) \times 10^{-3}$	1260 ± 65

superoxide-generating system, the concomitant formation of a carbon-centered radical adduct systematically occurred, as mentioned in the literature.[30,32] With the *tert*-butoxy radial ($tBuO^{\bullet}$), a second minor six-line species was also observed. According to Bors et al.,[33] this second species could arise from the *β*-scission of the *tert*-butoxy radical leading to methyl radical ($CH_3^{\bullet}$) which could react with O_2 to form a peroxy radical ($MeO_2^{\bullet}$).

The Fenton reaction was used to generate carbon-centered radicals, i.e., methyl, *α*-hydroxy radicals ($^{\bullet}CH_2OH$ and $CH_3CH^{\bullet}OH$), and 2-oxopropyl ($^{\bullet}CH_2C(O)CH_3$) radicals. Under these conditions, for all radicals generated, the main six line species were accompanied by a minor three-line species that could correspond to a nitroxide byproduct whose a_N value variation agreed well with the medium polarity.

In the absence of an $HO^{\bullet}$ scavenger, neither the Fenton system nor the photolysis of H_2O_2 led to the observation of the hydroxyl adduct, probably because of the very poor stability of hydroxyl radical adducts of PBN-type nitrones. Due to nitrone solubility issues, experiments were performed in the presence of $HO^{\bullet}$-unreactive cosolvents, i.e., dichloromethane or acetonitrile. Independent of the medium, only the weak three-line signal mentioned above, assigned to an unidentified nitroxide byproduct, was systematically observed (a_N = 14.4−14.6 G), along with the rather weak spectrum of a carbon-centered radical adduct exhibiting hfcc values of a_N = 13.2 G and a_H = 3.6 G for **3** in 55:45 ACN/H_2O (v/v) and a_N = 14.6 G and a_H = 3.4 G for **4** in 55:45 DCM/H_2O (v/v). These adducts could be formed via abstraction of a proton *α* to the carbonyl group of **3** and **4** by a $HO^{\bullet}$ radical and the subsequent trapping of radical with another molecule of **3** or **4**, thereby yielding the spin adducts denoted **3**-*3* and **4**-*4* (Scheme 2A).

Reduction of the nitronyl function using $NaBH_4$ led to the formation of the hydroxylamine form, which was further oxidized to the nitroxide according to the Forrester−Hepburn mechanism (Scheme 2B).[15] When compared to the literature,[34] both nitroxides exhibited expected a_N and a_H values for H-adducts derived from PBN-type nitrones; that is, a_N = 15.3 G and a_H = 9.7 G for nitrone **3** and a_N = 15.4 G and a_H = 10.3 G for nitrone **4**. In addition, the concomitant formation of a second nitroxide was systematically observed for all of the nitrones tested. The following hfcc values were determined for this second species: a_N = 15.4 G and a_H = 15.0 G for nitrone **3** and a_N = 15.4 G and a_H = 17.0 G for nitrone **4**. A survey of the spin-trapping literature clearly indicates that these species show a_H values that are much too high to be assigned to linear nitrone spin adducts and, therefore, may indicate the formation of 5-membered cyclic nitroxides. Although hypothetical, the formation of such cyclic nitroxides may arise from the basicity of the medium. Indeed, $NaBH_4$ contains NaOH and MeONa as impurities, which could promote the cyclization as depicted in Scheme 2B.

Kinetics of Spin-Adduct Decay. The light−riboflavin−DTPA system in DMSO was employed to investigate the kinetics of decay of the superoxide adduct. The decay was recorded after the irradiation was stopped, and the EPR signal persisted for 25−30 min. After deconvolution of the EPR spectra using the pseudoinverse procedure, the kinetic curves obtained were analyzed with a first-order decay fit (Figure 4). On the basis of the first-order rate constant determination, the half-life of the spin adducts was evaluated, and data are presented in Table 3. In agreement with the literature, the half-life of PBN is rather short ($t_{1/2}$ ∼3 min), while those of nitrone **3** and nitrone **4** are 2-fold longer, ∼5.5 and ∼6.7 min, respectively. A similar procedure was employed to study the decay of the hydroxymethyl spin adduct in a 6:4 methanol/H_2O mixture (v/v). A standard Fenton system was employed to generate $HO^{\bullet}$, which further reacted with methanol to yield $^{\bullet}CH_2OH$ radical. Only the spectra obtained after all of the Fenton system had been consumed (i.e., during the last 5 h) were considered in order to focus on the decay kinetics only. For all of the nitrones tested, hydroxymethyl spin adducts were

DOI: 10.1021/acs.joc.6b02262
J. Org. Chem. 2017, 82, 135−142

rather persistent with half-lives around 20 min, but no significant differences were observed between nitrones **3** and **4**, while PBN exhibited only a slightly shorter half-live ($t_{1/2}$ ~19 min for PBN/$^{\bullet}CH_2OH$ adduct vs ~21 min for **3**−CH_2OH and **4**−CH_2OH). In the next step, the persistence of the methyl radical adducts was examined in a 6:4 DMSO/H_2O mixture (v/v). A procedure similar to that used for the hydroxymethyl radical adducts was employed, with DMSO being used instead of methanol. All of the nitrones displayed an intense six-line signal corresponding to the methyl radical adduct, and no significant decrease occurred after 24 h in the EPR cavity. The three spin adducts showed a very high persistence in DMSO/H_2O since they were still detected after several days at room temperature. Notably, the decay of the three methyl adducts was not significantly faster after the addition of methanol (ca. 50% in volume) in the medium. This clearly indicates that the decay previously observed for the $^{\bullet}CH_2OH$ radical adducts did not correspond to the reduction of the nitroxide function by methanol. In view of the above findings, it can be concluded that the spin adducts of **3** and **4** were more persistent than that of PBN. This may originate from the steric hindrance associated with the cyclohexyl moiety, which could hamper the spin-adduct decay, although we cannot exclude electronic effects induced by the carboxylic acid.

CONCLUSION

We have synthesized a bifunctional α-phenyl-*N*-cyclohexyl-nitrone **4** containing a free carboxylic acid which is amenable to further functionalization. The synthesis is straightforward and allows the gram-scale preparation of paramagnetic impurity-free nitrone **4** in 61% overall yield in four steps. The water solubility of nitrone **4** is poor but can be significantly improved after conversion to the carboxylate salt. The presence of the cyclohexyl ring does not affect either the reduction or oxidation potentials of the nitronyl group when compared to the classical PBN, as demonstrated by cyclic voltammetry. Nitrone **4** showed efficient trapping of carbon- and oxygen-centered radicals, and the half-life of $^{\bullet}O_2H$ adducts was twice as long as that of PBN. This demonstrates that the cyclohexyl group significantly slows the spin-adduct decomposition, although further studies are required to elucidate if the carboxylic acid functionality has a significant effect.

EXPERIMENTAL SECTION

Synthesis. All reagents were from commercial sources and used as received. All solvents were distilled and dried according to standard procedures. TLC analysis was performed on aluminum sheets coated with silica gel (40−63 μm). Compound detection was achieved either by exposure to UV light (254 nm) and by spraying a 5% sulfuric acid solution in ethanol or a 2% ninhydrin solution in ethanol and then by heating at ~150 °C. Flash chromatography was carried out on silica gel (40−63 μm). Melting points have not been corrected. The ^{1}H NMR spectra were recorded at 400 MHz and the ^{13}C NMR at 100 MHz. Chemical shifts are given in ppm relative to the solvent residual peak as a heteronuclear reference for ^{1}H and ^{13}C. Abbreviations used for signal patterns are bs, broad singulet; s, singlet; d, doublet; dd, doublet of doublet; t, triplet; q, quartet; m, multiplet. HR-MS spectra were recorded on a mass spectrometer equipped with a TOF analyzer for ESI+ experiments.

Compound ***1***. Under argon atmosphere, 5 g (38.7 mmol, 1 equiv) of nitrocyclohexane were dissolved in Et_2O (8 mL). The solution was cooled, and 0.44 mL of a 1.5:8.5 KOH/MeOH solution (m/m) (1.11 mmol, 1/35 equiv) and 4.9 mL of *tert*-butoxy acrylate (38.7 mmol, 1 equiv) were successively added dropwise. The solution was stirred at RT for 16 h then AcOH was added until the pH of the solution reached ~5. The solvents were removed under vacuum, and the resulting crude residue was purified by flash chromatography (cyclohexane/Et_2O 95:5 v/v) to lead to compound **1** (8.95 g, 34.83 mmol, 90%) as a yellow oil: R_f (cyclohexane/Et_2O) = 0.37; ^{1}H NMR ($CDCl_3$, 400 MHz) δ 2.46−2.41 (2H, m), 2.22−2.14 (4H, m), 1.64−1.34 (8H, m), 1.46 (3H, s); ^{13}C NMR ($CDCl_3$, 100 MHz) δ 171.4, 91.3, 80.6, 35.0, 33.4, 29.5, 28.1, 24.5, 22.4; MS (ESI+, *m*/*z*) 258 [(M + H)$^+$], 275 [(M + NH_4)$^+$], 280 [(M + Na)$^+$], 296 [(M + K)$^+$]; HR-MS (ESI+, *m*/*z*) calcd for $C_{13}H_{23}O_4N$ [(M + H)$^+$] 258.1706, found 258.1715.

Compound ***2***. Under argon atmosphere, 1.89 g of compound **1** (6.60 mmol, 1 equiv) and 0.53 g of NH_4Cl (9.90 mmol, 1.5 equiv) were dissolved in a 3:1 THF/H_2O mixture (v/v). The solution was cooled, and 1.72 g of zinc dust (24.4 mmol, 4 equiv) was added portionwise, keeping the temperature below 15 °C during the addition, then the solution was stirred for 2 h at rt and filtered off through a pad of Celite. The solvents were removed under vacuum, and the crude residue was purified by flash chromatography (cyclohexane/EtOAc, 8:2 v/v) to lead to compound **2** (1.44 g, 5.28 mmol, 80%) as a white powder: R_f (cyclohexane/EtOAc, 8:2 v/v) = 0.22; ^{1}H NMR ($CDCl_3$, 400 MHz) δ 5.55 (1H, bs), 2.19 (2H, t, J = 6.0 Hz), 1.71 (2H, t, J = 6.0 Hz), 1.60−1.10 (10H, m), 1.39 (9H, s); ^{13}C NMR ($CDCl_3$, 100 MHz) δ 174.4, 80.2, 57.82, 32.5, 31.2, 29.4, 28.0, 25.9, 21.8; MS (ESI+, *m*/*z*) 244 [(M + H)$^+$], 266 [(M + Na)$^+$], 282 [(M + K)$^+$]; HR-MS (ESI+, *m*/*z*) calcd for $C_{13}H_{26}O_3N$ [(M + H)$^+$] 244.1913, found 244.1911.

Compound ***3***. Under argon atmosphere, 0.98 g of benzaldehyde (9.28 mmol, 1 equiv) and 1.81 g of compound **2** (7.38 mmol, 0.8 equiv) were dissolved in a 3:2 THF/AcOH mixture (v/v) in the presence of 4 Å molecular sieves. The solution was stirred at 60 °C for 16 h, and 0.25 equiv of compound **2** was added after 3 and 14 h of stirring (total mass of compound **2** 2.95g, 12.0 mmol, 1.3 equiv). The crude mixture was filtered through a pad of Celite, and the solvents were removed under vacuum. The resulting crude residue was purified by flash chromatography (cyclohexane/EtOAc, 8:2 v/v) to lead to compound **3** (2.83 g, 8.54 mmol, 92%) as a white powder: R_f (cyclohexane/EtOAc, 8:2 v/v) = 0.40; mp 154.8−157.6 °C; ^{1}H NMR ($CDCl_3$, 400 MHz) δ 8.29 (2H, m), 7.50−7.35 (4H, m), 2.30−2.10 (6H, m), 1.84 (2H, m), 1.61 (4H, m), 1.50 (2H, m), 1.40 (9H, s); ^{13}C NMR ($CDCl_3$, 100 MHz) δ 172.4, 131.7, 130.8, 130.2, 128.9, 128.5, 80.5, 75.2, 34.3, 29.6, 28.0, 25.4, 22.30; MS (ESI+, *m*/*z*) 332 [(M + H)$^+$], 354 [(M + Na)$^+$], 370 [(M + K)$^+$]; HR-MS (ESI+, *m*/*z*) calcd for $C_{20}H_{30}O_3N$ [(M + H)$^+$] 332.2226, found 332.2252.

Compound ***4***. Under argon atmosphere, 0.5 g of compound **3** (1.51 mmol) was dissolved in a 2:8 TFA/CH_2Cl_2 mixture (v/v). The solution was stirred for 4 h at rt, and then the solvents were removed under vacuum. The resulting crude mixture was purified by flash chromatography (EtOAc/cyclohexane, 6:4 v/v) to lead to compound **4** (0.38 g, 1.39 mmol, 92%) as a white powder: R_f (cyclohexane/EtOAc, 6:4 v/v) = 0.12; mp 187.8−189.2 °C; ^{1}H NMR ($CDCl_3$, 400 MHz) δ 8.29 (2H, m), 7.53 (1H, s), 7.44 (3H, m), 2.32−2.28 (2H, m), 2.21−2.17 (4H, m), 1.90−1.83 (2H, m), 1.63−1.58 (4H, m), 1.50 (2H, m); ^{13}C NMR ($CDCl_3$, 100 MHz) δ 176.6, 134.9, 131.3, 130.1, 129.8, 128.7, 75.5, 34.4, 32.6, 28.5, 25.5, 22.3; MS (ESI+, *m*/*z*) 276 [(M + H)$^+$], 298 [(M + NH_4)$^+$], 314 [(M + K)$^+$]; HR-MS (ESI+, *m*/*z*) calcd for $C_{16}H_{22}O_3N$ [(M + H)$^+$] 276.1600, found 276.1611

Determination of Water Solubility. For PBN and nitrones **3** and **4**, a UV-calibration curve at 290 nm was established from solutions ranging from 10^{-3} to 10^{-2} g/L (R^2 > 0.997). A saturated solution of nitrone was prepared at 40 °C and then allowed stand at rt overnight. After centrifugation (12000 g, 15 min) at rt, the concentration of the supernatant solution was determined using the calibration curve.

Determination of log k'_w Values. Compounds were dissolved in MeOH at 0.5 mg/mL and were injected onto a C18 reversed-phase column (250 mm × 4.6 mm, 5 μm). The compounds were eluted at various MeOH and water ratios (9:1 to 4:6 v/v) with 0.1% acetic acid using a flow rate of 0.8 mL/min. The column temperature was 25 °C, and the UV detector wavelength was λ = 298 nm. Linear regression analysis was performed on four data points for compound **3** (from 9:1 to 6:4; R^2 > 0.997); compound **4** (from 7:3 to 4:6; R^2 > 0.999) and

DOI: 10.1021/acs.joc.6b02262
J. Org. Chem. 2017, 82, 135−142

PBN (from 7:3 to 4:6; $R^2 > 0.999$). The log k' values were calculated by using the equation: $\log k' = \log((t - t_0)/t_0)$, where t is the retention time of the nitrone and t_0 is the elution time of MeOH, which is not retained on the column.

Determination of *C* log *P* Values. The partition coefficient octanol/water (Clog*P*) was determined using MarvinSketch 5.9.0, which is available at www.chemaxon.com/marvin.

Cyclic Voltammetric Measurement. The electrochemical experiments were carried out using a three-electrode cell in a dry argon atmosphere at room temperature. An Ag/AgCl/saturated NaCl electrode was used as the reference electrode and a platinum wire as the auxiliary electrode. The working electrode (glassy carbon) was polished prior to each experiment using a 0.04 μm aqueous alumina slurry on a wetted polishing cloth.

Spin-Trapping Experiments. Free radicals were produced in the presence of the nitrone of interest (50−100 mmol L^{-1}) solubilized in organic solvents. EPR assays were carried out in capillary tubes. EPR spectra were recorded at room temperature on an X-band Bruker EMX spectrometer equipped with an NMR gaussmeter for magnetic field calibration. The following conditions were used: modulation frequency, 100 kHz; nonsaturating microwave power, 10−15 mW; modulation amplitude, from 0.1 to 0.125 mT; receiver gain, from 5×10^3 to 5×10^5; time constant, from 1.28 to 655 ms; scan time, from 60 to 180 s; scan width, from 4.5 to 7 mT. Standard EPR simulations were performed using Winsim software elaborated by Duling and provided by the National Institute of Environmental Health Sciences.[35]

Carbon-Centered Radicals. The carbon-centered radicals $^{\bullet}CH_2C(O)CH_3$, $^{\bullet}CH_2OH$, $^{\bullet}CH(CH_3)OH$, and $^{\bullet}CH_3$ were generated by using acetone, methanol, ethanol, or DMSO, respectively. In all experiments, the medium contained 60% of organic solvent used as the $HO^{\bullet}$ scavenger.

tert-Butoxy Radical. The *tert*-butoxy radical $tBuO^{\bullet}$ was generated in the presence of the nitrone by UV photolysis of a 3 mol·L^{-1} $(OtBu)_2$. Benzene was used with nitrone **4**, while dichloromethane was employed with nitrone **3**.

Methoxy Radical. The methoxyl radical was produced in methanol by adding $Pb(OAc)_4$ (10 mmol L^{-1}) to a 50 mmol L^{-1} nitrone solution in methanol.

Superoxide Radical. The superoxide radical was produced in DMSO in the presence of 100 mmol L^{-1} nitrone by irradiating a solution containing 0.1 mmol L^{-1} riboflavin and 4 mmol L^{-1} ethylenetriaminepentacetic acid (DTPA) with blue light. In these experiments, the medium was irradiated directly into the cavity of the EPR spectrometer.

Hydroxyl Radical. The hydroxyl radical was generated in the presence of the nitrone by a Fenton system consisting of 0.4% H_2O_2 and 10 mmol L^{-1} $FeSO_4$. Stock solutions of both H_2O_2 and $FeSO_4$ were prepared in water, while the nitrone was solubilized in either DCM or DCM/ACN (1/4 vol/vol). In a standard experiment, $FeSO_4$ and the nitrone of interest were mixed together before H_2O_2 addition, and the medium was immediately transferred in a capillary tube for EPR analysis.

H-adducts. The "pseudo H-adducts" were obtained by reducing the two nitrones (0.1 mol·L^{-1}) by $NaBH_4$ (0.3 mol·L^{-1}) in methanol. Autoxidation of the hydroxylamines led to the corresponding aminoxyl radicals.

Spin Adduct Persistence. The persistence of superoxide, hydroxymethyl, and methyl radical adducts was examined in organic media. Kinetic studies of the decay of the nitrone−superoxide adducts were carried out using the light−riboflavin system described above to generate superoxide in the presence of 100 mmol L^{-1} nitrone. The medium was irradiated with blue light directly into the EPR cavity for 2−3 min, and the light was shut off before recording a series of EPR spectra for at least 30 min. One spectrum was then recorded every 20 s in order to collect a series of at least 100 spectra for each experiment. Using a procedure fully described elsewhere,[36] noise was then reduced using the SVD procedure and the deconvolution using the pseudoinverse method was applied, thereby yielding the kinetic curves. After computer modeling of these curves considering an exponential decay, the value of the first-order kinetic constants k_D was obtained.

The same procedure was employed to study the decay of the CH_2OH spin adduct in a 6:4 methanol/water mixture (v/v). The hydroxymethyl radical was generated in the presence of 100 mmol L^{-1} nitrone by a standard Fenton system. The medium was transferred into a capillary tube placed in the spectrometer cavity, and one spectrum was recorded every 42 s during 15 h. Only the spectra obtained during the last 5 h (i.e., when we were sure that the $^{\bullet}OH$ production was over) were kept for the decay kinetic study. The same procedure was applied to examine the stability of the $^{\bullet}CH_3$ radical adducts by replacing the methanol by DMSO. All of the kinetic experiments were performed in duplicate.

■ ASSOCIATED CONTENT

Supporting Information

The Supporting Information is available free of charge on the ACS Publications website at DOI: 10.1021/acs.joc.6b02262.

^1H and ^{13}C NMR spectra and mass spectrometry data of compounds **1**−**4**; HPLC chromatogram (PDF)

■ AUTHOR INFORMATION

Corresponding Author

*E-mail: gregory.durand@univ-avignon.fr. Tel: +33 (0)4 9014 4445.

ORCID

Grégory Durand: 0000-0001-6680-2821

Notes

The authors declare no competing financial interest.

■ ACKNOWLEDGMENTS

M.R. was the recipient of a fellowship from "Région Provence Alpes Côte d'Azur". This work was supported by the University of Avignon and by a grant from the "Structure Fédérative de Recherche" TERSYS. We thank Quentin Hericher and Djilali Lahouel for excellent preliminary work on the synthesis of the compounds. B.T. acknowledges NIEHS for providing the Winsim software used to simulate the EPR spectra. We thank Dr. Lindon Moodie (Umeå University) for carefully proofreading the manuscript and Anaïs Delétraz for technical assistance.

■ REFERENCES

(1) Hawkins, C. L.; Davies, M. J. *Biochim. Biophys. Acta, Gen. Subj.* **2014**, *1840*, 708.

(2) Villamena, F. A.; Zweier, J. L. *Antioxid. Redox Signaling* **2004**, *6*, 619.

(3) Floyd, R. A.; Kopke, R. D.; Choi, C.-H.; Foster, S. B.; Doblas, S.; Towner, R. A. *Free Radical Biol. Med.* **2008**, *45*, 1361.

(4) Villamena, F. A.; Das, A.; Nash, K. M. *Future Med. Chem.* **2012**, *4*, 1171.

(5) Durand, G. In *Molecular Basis of Oxidative Stress*; John Wiley & Sons, Inc.: 2013; p 377.

(6) Rosselin, M.; Poeggeler, B.; Durand, G. *Curr. Top. Med. Chem.* **2016**, in press.

(7) Fréjaville, C.; Karoui, H.; Tuccio, B.; Moigne, F. L.; Culcasi, M.; Pietri, S.; Lauricella, R.; Tordo, P. *J. Med. Chem.* **1995**, *38*, 258.

(8) Olive, G.; Mercier, A.; Le Moigne, F.; Rockenbauer, A.; Tordo, P. *Free Radical Biol. Med.* **2000**, *28*, 403.

(9) Zhao, H.; Joseph, J.; Zhang, H.; Karoui, H.; Kalyanaraman, B. *Free Radical Biol. Med.* **2001**, *31*, 599.

(10) Villamena, F. A.; Rockenbauer, A.; Gallucci, J.; Velayutham, M.; Hadad, C. M.; Zweier, J. L. *J. Org. Chem.* **2004**, *69*, 7994.

(11) Villamena, F. A.; Xia, S.; Merle, J. K.; Lauricella, R.; Tuccio, B.; Hadad, C. M.; Zweier, J. L. *J. Am. Chem. Soc.* **2007**, *129*, 8177.

DOI: 10.1021/acs.joc.6b02262
J. Org. Chem. 2017, 82, 135−142

(12) Karoui, H.; Nsanzumuhire, C.; Le Moigne, F.; Hardy, M.; Siri, D.; Derat, E.; Rockenbauer, A.; Ouari, O.; Tordo, P. *Chem. - Eur. J.* **2014**, *20*, 4064.
(13) Allouch, A.; Roubaud, V.; Lauricella, R.; Bouteiller, J.-C.; Tuccio, B. *Org. Biomol. Chem.* **2003**, *1*, 593.
(14) Allouch, A.; Roubaud, V.; Lauricella, R.; Bouteiller, J.-C.; Tuccio, B. *Org. Biomol. Chem.* **2005**, *3*, 2458.
(15) Roubaud, V.; Lauricella, R.; Bouteiller, J.-C.; Tuccio, B. *Arch. Biochem. Biophys.* **2002**, *397*, 51.
(16) Durand, G.; Choteau, F.; Pucci, B.; Villamena, F. A. *J. Phys. Chem. A* **2008**, *112*, 12498.
(17) Rosselin, M.; Choteau, F.; Zéamari, K.; Nash, K. M.; Das, A.; Lauricella, R.; Lojou, E.; Tuccio, B.; Villamena, F. A.; Durand, G. *J. Org. Chem.* **2014**, *79*, 6615.
(18) Rosselin, M.; Tuccio, B.; Villamena, F. A.; Perio, P.; Fabre, P.-L.; Durand, G. *Electrochim. Acta* **2016**, *193*, 231.
(19) Thomas, C. E.; Ohlweiler, D. F.; Carr, A. A.; Nieduzak, T. R.; Hay, D. A.; Adams, G.; Vaz, R.; Bernotas, R. C. *J. Biol. Chem.* **1996**, *271*, 3097.
(20) Fevig, T. L.; Bowen, S. M.; Janowick, D. A.; Jones, B. K.; Munson, H. R.; Ohlweiler, D. F.; Thomas, C. E. *J. Med. Chem.* **1996**, *39*, 4988.
(21) Sár, C. P.; Hideg, É.; Vass, I.; Hideg, K. *Bioorg. Med. Chem. Lett.* **1998**, *8*, 379.
(22) Hideg, E.; Takátsy, A.; Sár, C. P.; Vass, I.; Hideg, K. *J. Photochem. Photobiol., B* **1999**, *48*, 174.
(23) Porcal, W.; Hernández, P.; González, M.; Ferreira, A.; Olea-Azar, C.; Cerecetto, H.; Castro, A. *J. Med. Chem.* **2008**, *51*, 6150.
(24) Soto-Otero, R.; Méndez-Álvarez, E.; Sánchez-Iglesias, S.; Labandeira-García, J. L.; Rodríguez-Pallares, J.; Zubkov, F. I.; Zaytsev, V. P.; Voskressensky, L. G.; Varlamov, A. V.; de Candia, M.; Fiorella, F.; Altomare, C. *Arch. Pharm.* **2012**, *345*, 598.
(25) Han, Y.; Tuccio, B.; Lauricella, R.; Rockenbauer, A.; Zweier, J. L.; Villamena, F. A. *J. Org. Chem.* **2008**, *73*, 2533.
(26) Kolter, T.; van Echten-Deckert, G.; Sandhoff, K. *Tetrahedron* **1994**, *50*, 13425.
(27) Durand, G.; Poeggeler, B.; Ortial, S.; Polidori, A.; Villamena, F. A.; Böker, J.; Hardeland, R.; Pappolla, M. A.; Pucci, B. *J. Med. Chem.* **2010**, *53*, 4849.
(28) Choteau, F.; Tuccio, B.; Villamena, F. A.; Charles, L.; Pucci, B.; Durand, G. *J. Org. Chem.* **2012**, *77*, 938.
(29) McIntire, G. L.; Blount, H. N.; Stronks, H. J.; Shetty, R. V.; Janzen, E. G. *J. Phys. Chem.* **1980**, *84*, 916.
(30) Tuccio, B.; Lauricella, R.; Frejaville, C.; Bouteiller, J.-C.; Tordo, P. *J. Chem. Soc., Perkin Trans. 2* **1995**, 295.
(31) Zuman, P.; Exner, O. *Collect. Czech. Chem. Commun.* **1965**, *30*, 1832.
(32) Buettner, G. R.; Oberley, L. W. *Biochem. Biophys. Res. Commun.* **1978**, *83*, 69.
(33) Bors, W.; Michel, C.; Stettmaier, K. *J. Chem. Soc., Perkin Trans. 2* **1992**, 1513.
(34) Buettner, G. *Free Radical Biol. Med.* **1987**, *3*, 259.
(35) Duling, D. R. *J. Magn. Reson., Ser. B* **1994**, *104*, 105.
(36) Lauricella, R.; Allouch, A.; Roubaud, V.; Bouteiller, J.-C.; Tuccio, B. *Org. Biomol. Chem.* **2004**, *2*, 1304.

DOI: 10.1021/acs.joc.6b02262
J. Org. Chem. 2017, 82, 135−142